How active site protonation state influences the reactivity and ligation of the heme in chlorite dismutase

Bennett R. Streit,[1] Béatrice Blanc,[1] Gudrun S. Lukat-Rodgers,[2] Kenton R. Rodgers,[2] Jennifer L. DuBois[1]

Contents:

Figure S1. Change in UV/visible absorbance upon changing pH from 6.8 (dashed line) to 4 (solid black line). Scans were taken at 3 s intervals after changing the pH from 6.8 to 4 by addition of a concentrated 100 mM citrate phosphate buffer, pH 3.2. All spectra were corrected for dilutions. The inset shows the absorbance at 393 as a function of time.

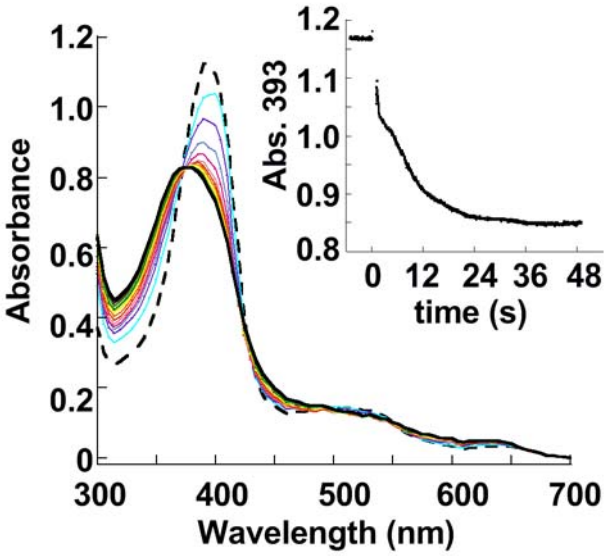

Figure S2. Correlation between the change in absorbance of Soret band at 393 nm and rate of chlorite dismutation upon change of pH from 6.8 to 4. To normalize the change in ΔAbsorbance or change in $[O_2]$ concentration, the ΔAbs at time t (ΔAbs_t) or the $[O_2]$ at time t ($[O_2]_t$) is divided by either the ΔAbsorbance or $[O_2]$ at the final time point (ΔAbs_f or $[O_2]_f$). The time course of the O_2-evolution reaction, which does not go to completion, matches that of the Soret band's blue shift. This suggests that the reaction continues only as long as active enzyme is available.

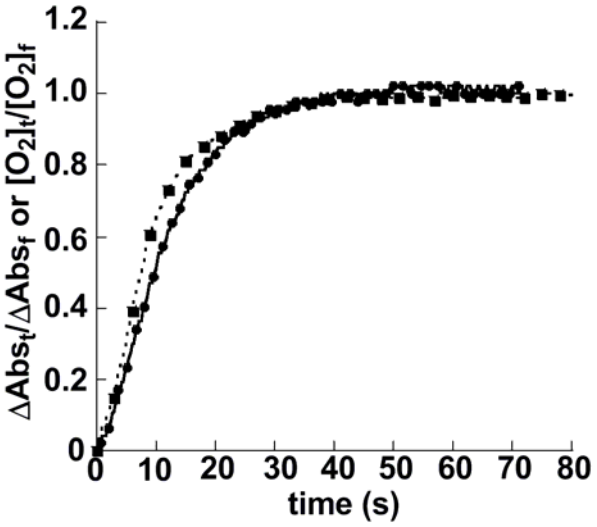

Figure S3.

(a)The Cld UV/vis spectrum was titrated from 6.7 (dashed line) to 9.5 (solid black line) at 25°C in 100 mM citrate-phosphate buffer. This buffer was used for all of the steady-state kinetic data reported in the text. The inset shows the absorbance at 393 as a function of pH with a pKa of 8.9±0.2. The peak maxima isosbestic points, and pK_a are all identical to what was measured in the 20mM (each) Mes/Ches/Tris mixed buffer reported in the text. Spectra were obtained at pH 6.7 (Soret band at 393 nm), 7, 7.5, 7.9, 8.2, 8.6, 9 and 9.5 (Soret band at 410 nm). As the pH increases above 9.5, the Soret absorbance begins to blue shift due to formation of a new 5cHS species presumed to be due to loss of axial His ligation and coordination of OH at the distal side. The spectrum at pH 6.7 shows a Soret band at 393 nm and CT bands at 644 nm and 509 nm respectively. At pH 9.5, the spectrum shows a Soret band at 410 nm, and α and β at 576 nm and 533 nm respectively. The isosbestic points for the transition of the 5c-HS species to the 6c species occur at approximately 351 nm, 469 nm, 540 nm, 558 nm, 621 nm. Discrepancies in the isosbestic points are likely due to small shifts in the UV/vis baseline that occurred following removal and refilling of the spectrometer cuvette.

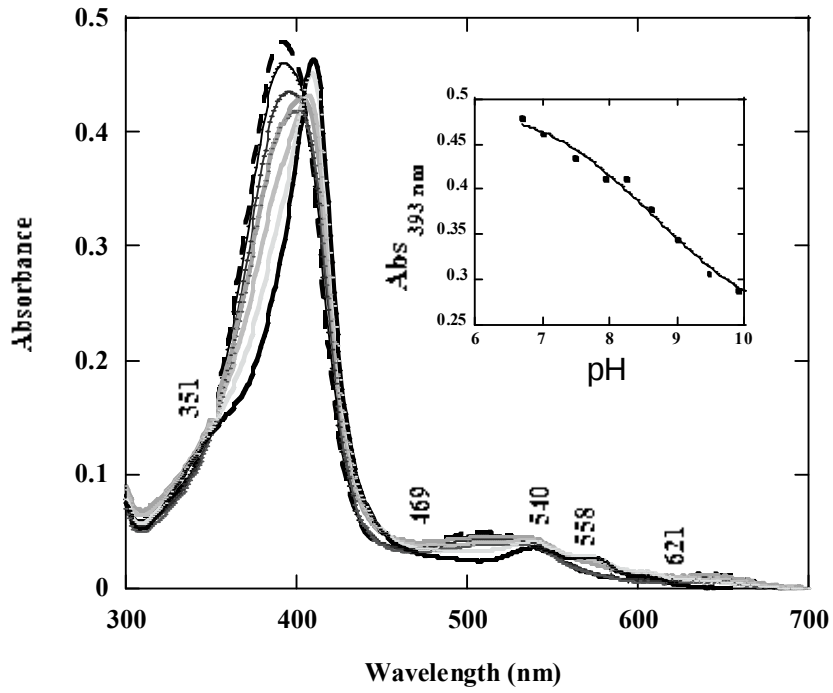

Figure S4. High frequency rR spectra of ferrous Cld at pH 5.8, 6.8, 7.5, and 10.0. Spectra were acquired with 406.7 nm excitation (18 mW). Solutions at pH 6.8 and 7.5 were buffered in 100 mM sodium phosphate. The pH 5.8 and 10.0 solutions were buffered with 100 mM sodium citrate and Ches, respectively. The asterisks mark intensity due to Hg atomic emission from inadvertent and indirect exposure of the spectrometer to ambient fluorescent lighting.

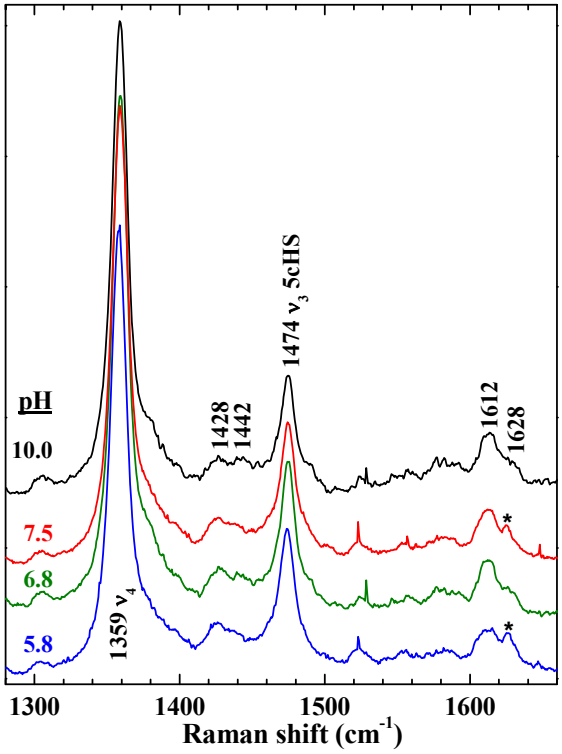

Figure S5. Soret-excited (413.1 nm) rR spectra of Cld−CO (black) and Cld−^{13}CO (red), along with the respective difference spectra (blue) as a function of pH. The difference spectra reveal the isotope-sensitivities of the ν_{Fe-C} and ν_{C-O} bands. They further reveal two forms of Cld−CO whose relative populations are sensitive to pH. The FeCO features attributable to form 1 have greater amplitude than those of form 2. However form 1 is more favored at high pH than it is at low pH. Bands arising from FeCO vibrations are labled in blue and were assigned based on their ^{13}CO isotope shifts. Iron porphyrinate bands are labeled in green.

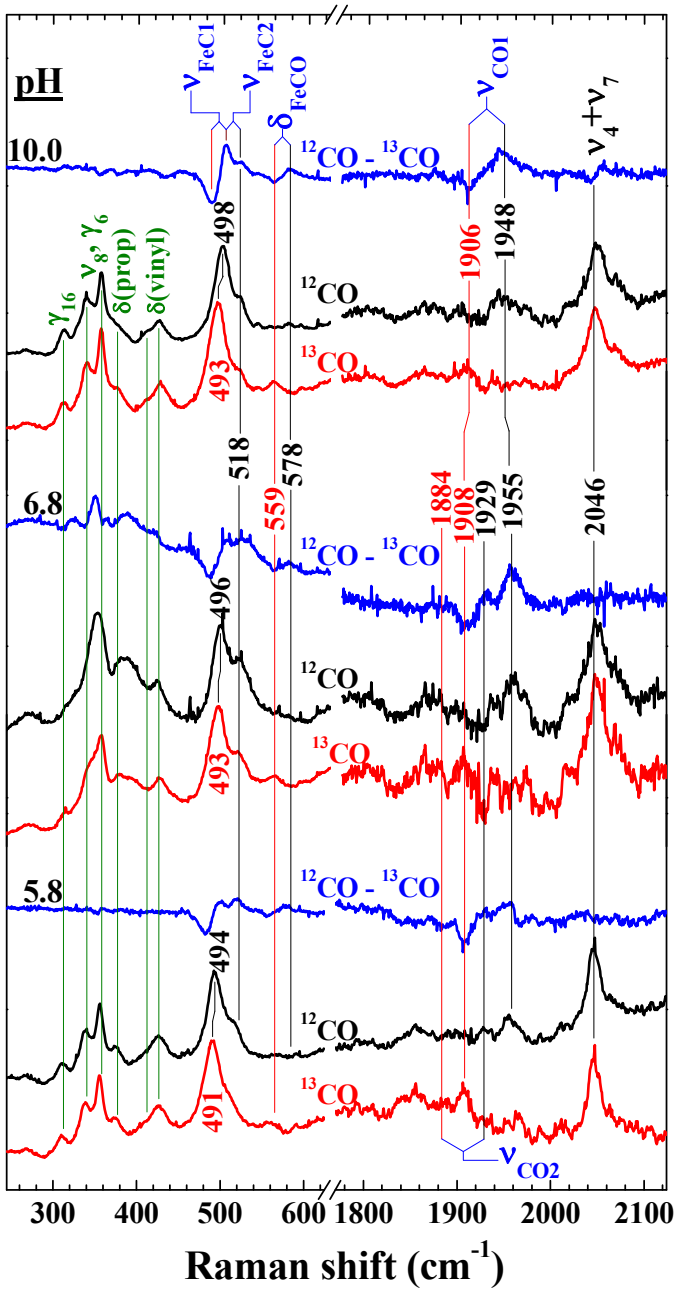

Figure S6. Spectra of ligand-bound Cld. Spectra were measured at ligand concentrations and pH values ensuring full occupation of the Fe sites. The visible region of the spectrum (450 -800 nm) is magnified 10 fold for clarity. (a) oxidized Cld; (b) cyanide bound spectrum; (c) azide bound spectrum; (d) fluoride bound spectrum; (e) nitrite bound spectrum; (f) pyridine bound spectrum; (g) thiocyanate bound spectrum; (h) imidazole bound spectrum. Peak positions are indicated on Table 2 in the text.

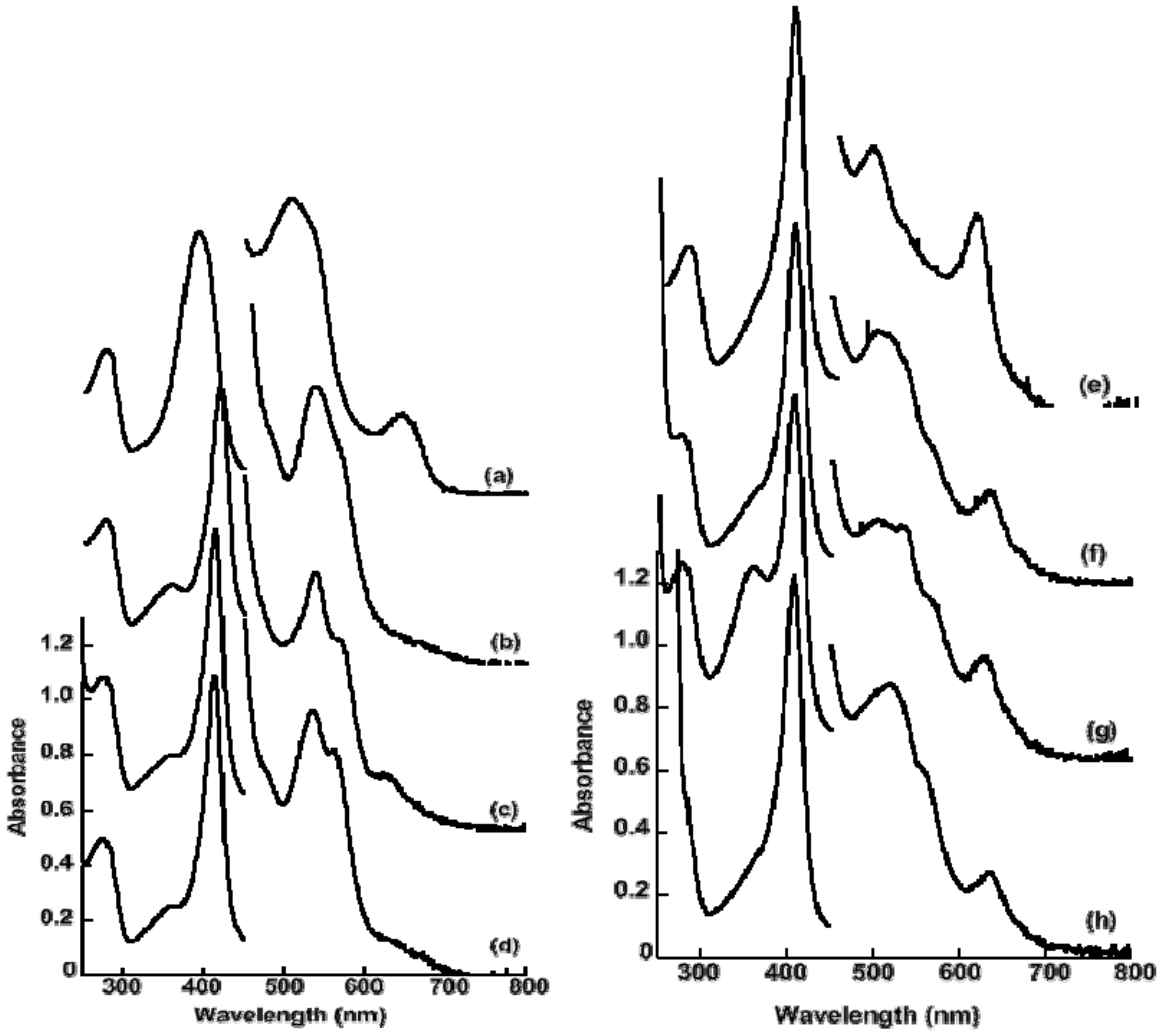

Figure S7. Soret-excited rR spectra of ferric Cld complexes: Cld−CN^- (4.5 mM NaCN, pH 7.0), Cld−ImH (1.2 mM imidazole, pH 7.5), Cld−N_3^- (2.0 mM NaN_3, pH 7.5), Cld−NO_2^- (11 mM $NaNO_2$, pH 6.8), Cld−SCN^- (9.8 mM KSCN, pH 5.8), and Cld−F^- (1.3 M NaF, pH 5.8). These complexes were prepared at the pH of their greatest thermodynamic stability in the presence of saturating exogenous ligand concentrations, as determined by spectrophotometric titrations (see Figure 7). The Cld−CN^- and Cld−ImH complexes are completely 6c and LS. The Cld−N_3^-, Cld−NO_2^-, and Cld−SCN^- complexes harbor equilibrium mixtures of 6cHS and 6cLS hemes. The Cld−F^- complex is 6cHS.

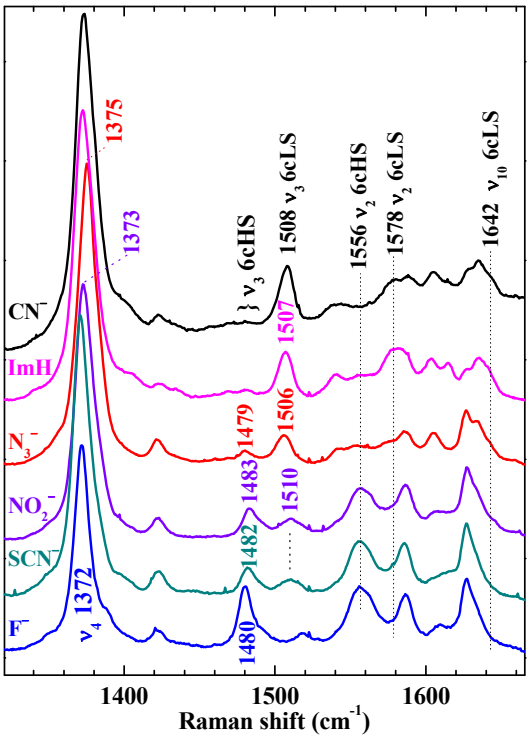

Figure S8. Representative plots illustrating data quality and analysis for Cld/ligand binding titrations. (a) Titration of imidazole at pH 7.0 in a 10 mM phosphate buffer. Spectra were measured after imidazole additions of 0, 4.84, 9.38, 13.7, 17.6, 21.4, 25.0, 28.4, 47.4, 65.4, 82.5, 446, and 793 μM. Spectra are corrected for dilution. The inset shows an expanded view of the visible region of the spectrum. (b) Difference plot generated from (a). (c) Plot of ΔAbs_{385} as a function of ligand concentration. The inset shows an expanded view of the initial changes in absorbance as a function of pH. The data were fit to an equilibrium isotherm, as described in the text.

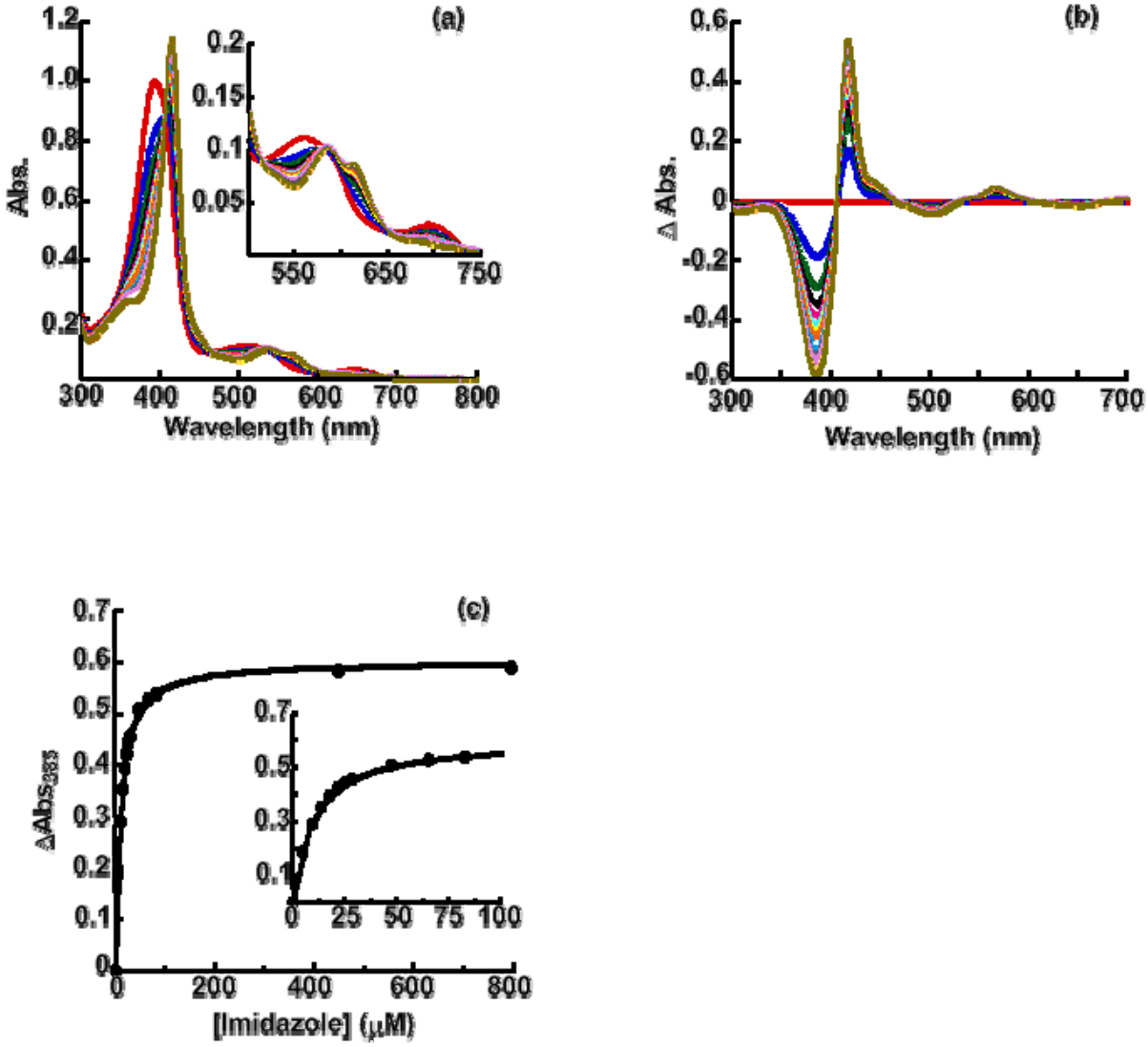

Table S1. Frequencies for Ferrous CO complexes of heme proteins

Fe(II)-CO	νFe−C	νC−O	δFe−C−O	Reference
Cld pH 6.8	496	1957	575	this work
Cld pH 10.0	499	1945	576	this work
Sensor Proteins				
sGC	472	1987	562	1
*Ec*Dos	486	1973	nr	2
*Ec*DosH	487	1969	575	3
CooA	487	1982	nr	4
*Ax*PDEA1H	493	1973	581	3
HemAT-B	494	1964	573	5
*Mt*DosH	494	1972	570	3
NPAS2 bHLH-PAS-A	495	1962	nr	6
NPAS2 PAS-A	496	1962	572	7
*Bj*FixL	496	1969	571	3
sGC	497	1959	574	8, 9
NPAS2 PAS-B	497	1962	577	10
CLOCK PAS-A	498	1960	576	submitted
*Rm*FixLH	498	1962	576	11
CooA(alkaline)	500	1964	nr	4
*Rm*FixLT	502	1956	572	11
Peroxidases/catalases				
HRP(I)	490	1932		12
CCP(I)	495	1922		13
KatG	499	1965	no	14
HRP(III)	516	1933		15, 16
KatG	522	1926	584	14
CCP(II)	530	1922		13
HRP(II)	539	1906		12,16,15
Catalase	542	1908		17
Heme Transport proteins				

PhuS	498	1960	578	18
ShuS	498	1964	582	unpublished results
*Sm*HasA	532	1954		19
Globins				
SW myoglobin	507	1947		20, 21
human myoglobin	508	1941		22, 23
M. tuberculosis HbN	500	1948		24
	534	1917		24
Ascaris suum Hb	543	1909	588	25
	515	1948		25
Models				
PPDMe(Im^{-})	490	1942		12
PPMeImH	495	1960		12

Table S2. UV/Visible bands and spin states for several heme proteins and their hydroxide complexes

Protein	Sixth ligand	Soret	CT1	β	α	CT2	Spin	Ref
HRP (pH <3.1)	H_2O*	370	-	515	-	652	hs	[26]
HRP(neutral)	none	403	497	-	-	641	hs	[27]
HRP (pH 11)	OH^-	416	-	545	575	-	ls	[27]
CCp (neutral)	none	408	508	540	592	644	hs	[28]
CCp (pH 8)	His	414	488	534	563	629	ls	[28]
HRP(H42R)	OH^-	408	498	538	575	607 (643)	mixed	[29]
CCp(D235N)	none	406	500	535	576	624	hs	[28]
CCp(D235N)	OH^-	412	503	541	576	627	ls	[28]
CCp(D235N)	His	414	485	531	566	634	ls	[28]
swMb (pH 4)	H_2O *	370		510		641	hs	[26]
swMb (neutral)	H_2O	409.5	505	546	590	635	hs	[30,31]
swMb (pH < 11)	OH^-	414	484	542	582	595	mixed	[30,31]
CIP (pH 3.8)	H_2O*	394	-	507		652	hs	[26]
CIP (neutral)	none	403	-	505	534	649	hs	[26]
CIP (pH 12.1)	OH^-	412 (370sh)	-	543	575	-	ls	[26]
CIP(D245N) (pH3.8)	H_2O	412 (370)	506	534	575	639	hs (hs*)	[26]
CIP(D235N) (neutral)	H_2O	407	502	536	575	639	hs	[26]
CIP(245N) (pH 10)	OH^-	410 (370)	(511)	541	575	(644)	hs (hs*)	[26]

[a] Phosphate buffer; [b] nitrate buffer; * coordination of water or hydroxide, but loss of proximal His ligation.

Sample equation derivation

A derivation of the equation describing the pH dependence of k_{cat}/K_m exhibiting 3 pK_as (model 1, equation (7) in text) is shown:

A 3 pK_a model implies that there are at least four different enzyme forms separated by the 3 turning points on the k_{cat}/K_m plot:

$$k_{cat}/K_m\ (obs) = c[EH_2]/[E_t] + c'[EH]/[E_t] \qquad \text{(Eq.S1)}$$

In the present case, the enzyme forms EH_2 and EH are active. EH_3 and E are not active. Therefore, at any pH, the observed k_{cat}/K_m is a function of the proportion of enzyme in the EH_2 form and its intrinsic k_{cat}/K_m (called c) and the EH form and its intrinsic k_{cat}/K_m (c'). :

$$k_{cat}/K_m\ (obs) = c[EH_2]/[E_t] + c'[EH]/[E_t] \qquad \text{(Eq.S2)}$$

With three pK_as, the total enzyme concentration E_t will be partitioned according to the pH of the solution:

$$E_T = EH_3 + EH_2 + EH + E \qquad \text{(Eq.S3)}$$

Partitioning of the enzyme between the 4 forms will be determined by the three K_as according to:

$$\mathbf{Ka(1)} = \frac{\mathbf{[EH_2][H^+]}}{\mathbf{[EH_3]}}, \mathbf{Ka(2)} = \frac{\mathbf{[EH][H^+]}}{\mathbf{[EH_2]}}, \mathbf{Ka(3)} = \frac{\mathbf{[E][H^+]}}{\mathbf{[EH]}} \qquad \text{(Eq. S4 - S6)}$$

These K_a expressions are rearranged and used to express $[E_T]$ in terms of the concentration of each enzyme species in the numerator terms of Eq.S2. For example:

$[EH_3] = [EH_2][H^+]/K_a(1)$

$[EH] = K_a(2)\ [EH_2]/[H^+]$

$[E] = K_a(3)[EH]/[H^+] = K_a(2)xK_a(3)\ [EH_2]/[H^+]^2$

And $[E_T] = [EH_2][H^+]/K_a(1) + [EH_2] + K_a(2)\ [EH_2]/[H^+] + K_a(2)xK_a(3)\ [EH_2]/[H^+]^2$

A similar expression can be written in terms of [EH]. These expressions for $[E_T]$ are substituted back into Eq.S2 to give the expression:

$$k_{cat}/K_m\ (obs) = \left\{ \frac{c}{1 + \frac{Ka(2) \times Ka(3)}{[H^+]^2} + \frac{[H^+]}{Ka(1)} + \frac{Ka(2)}{[H^+]}} + \frac{c'}{1 + \frac{[H^+]}{Ka(2)} + \frac{Ka(3)}{[H^+]} + \frac{[H^+]^2}{Ka(1) \times Ka(2)}} \right\}$$

Taking the logarithm of both sides gives equation (7). The other equations expressing the pH dependence of kinetic parameters or K_D were derived in an analogous way.

References

(1) Tomita, T.; Ogura, T.; Tsuyama, S.; Imai, Y.; Kitagawa, Y. *Biochemistry* **1997**, *36*, 10155-10160.

(2) Sato, A.; Sasakura, Y.; Sugiyama, S.; Shimizu, T.; Mizutani, Y.; Kitagawa, T. *Journal of biological chemistry* **2002**, *277*, 32650-32658.

(3) Tomita, T.; Gonzalez, G.; Chang, A.L.; Ikeda-Saito, M.; Gilles-Gonzales, M.A. *Biochemistry* **2002**, *41*, 4819-4826.

(4) Coyle, C.M.; Puranik, M.; Youn, H.; Nielsen, S.B.; Wiliams, R.D., Kerby, R.L.; Roberts, G.P.; Spiro, T.G. *Journal of biological chemistry* **2003**, *278*, 35384-35393.

(5) Aono S., Kato, T., Matsuki, M., Nakajima, H. Ohta, T., Uchida, T., Kitagawa, T. **2002** *Journal of biological chemistry, 277*, 13528-13538.

(6) Mukaiyama, Y.; Uchida, T.; Sato, E.; Sasaki, A.; Sato, Y.; Igarashi, J.; Kurokawa, H.; Sagami, I.; Kitagawa, T.; Shimizu, T. *FEBS journal* **2006**, *273*, 2528-2539.

(7) Uchida, T.; Sato, E.; Sato, A.; Sagami, I.; Shimizu, T.; Kitagawa, T. *Journal of biological chemistry* **2005**, *280*, 21358-21368.

(8) Yu A.E.; Hu, S.; Spiro, T.G., Burstyn, J.N. *Journal of the American Chemical Society* **1994**, *116*, 4117-4418.

(9) Fan, B.; Gupta, G.; Danziger, R.S.; Friedman, J.M.; Rousseau, D.L. *Biochemistry* **1998**, *37*, 1178-1184.

(10) Koudo, R.; Kurokawa, H.; Sato, E.; Igarashi, J.; Uchadi, T.; Sagamu, I.; Kitagawa,T.; Shimizu, T. *FEBS journal* **2005**, *272*, 4153-4162.

(11) Miyatake, H.; Mukai, M., Adachi, S.I.; Nakamura, H.; TAmura, K.; Iizuka, T.; Shiro, Y.; Strange, R.W.; Hasnain, S.S. *Journal of biological chemistry* **1999**, *274*, 23176-23184.

(12) Evangelista-kirkup, R.; Smulevich, G.; Siro, T.G. *Biochemistry* **1986**, *25*, 4420-4425.

(13) Li, X. Y.; Spiro, T. G. *J. Am. Chem. Soc.* **1988**, *110*, 6024-6033.

(14) Lukat-Rodgers, G.S.; Wengenack, N.L.; Rusnak, F.; Rodgers, K.R. *Biochemistry* **2001**, *40*, 7149-7157.

(15) Uno, T.; Nishimura, Y.; Tsuboi, M.; Makino, R.; Iizuka, T.; Ishimura, Y. *Journal of biological chemistry* **1987**, *262*, 4549-4556.

(16) Feis, A.; Rodriguez-Lopez, J.N.; Thorneley; R.N.F.; Smulevich, G. *Biochemistry* **1998**, *37*, 13575-13581.

(17) Hu, S.; Kincaid, J.R. *FEBS letters* **1992**, *314*, 293-296.

(18) Block, D.R.; Lukat-Rodgers, G.S.; Rodgers, K.R.; Wilks, A.; Bhata, M.N.; Lansky, I.B. *Biochemistry* **2007**, *46*, 14391-14402.

(19) Lukat-Rodgers, G. S.; Rodgers, K. R.; Caillet-Saguy, C.; Izadi-Pruneyre, N.; Lecroisey, *Biochemistry* **2008**, *47*, 2087-2098.

(20) Anderton, C.L.; Hester, R.E.; Moore, J.N. *Biochimica et Biophysica Acta* **1997**, *1338*, 107-120.

(21) Spiro, T.G.; Wasbotten, I.H. *Journal of inorganic biochemistry* **2005**, *99*, 34-44.

(22) Ling, J.; Li. T.; Oslon, J.S.; Bocian, D.F. *Biochimica et biophysica acta.* **1994**, *1188*, 417-421.

(23) Li, T.; Quillin, M.L.; Phillips, G.N., Jr, Olson, J.S. *Biochemistry* **1994**, *33*, 1433-1446.
(24) Yeh, S.R.; Couture, M.; Oullet, Y.;Guertin, M.; Rousseau, D.L. *Journal of biological chemistry* **2000**, *275*, 1679-1684.
(25) Das, T.K.; Friedman, J.M.; Kloek, A.P.; Goldberg, D.E.; Rousseau, D.L. *Biochemistry* **2000**, *39*, 837-842.
(26) Smulevich, G.; Neri, F.; Marzocchi, M. P.; Welinder, K. G. *Biochemistry* **1996**, *35*, 10576-10585.
(27) Keilin, D.; Hartree, E. F. *Biochem. J.* **1951**, *49*, 88-106.
(28) Vitello, L. B.; Erman, J. E.; Miller, M. A.; Mauro, J. M.; Kraut, J. *Biochemistry* **1992**, *31*, 11524-11535.
(29) Howes, B. D.; RodriguezLopez, J. N.; Smith, A. T.; Smulevich, G. *Biochemistry* **1997**, *36*, 1532-1543.
(30) Hanania, G. I.; Yeghiayan, A.; Cameron, B. F. *Biochem. J.* **1966**, *98*, 189-192.
(31) Smith, D. W.; Williams, R. J. *Biochem. J.* **1968**, *110*, 297-301.